Membrane Fusion by Influenza Hemagglutinin

J.J. SKEHEL,[1] T. BIZEBARD,[2] P.A. BULLOUGH,[3] F.M. HUGHSON,[3] M. KNOSSOW,[2] D.A. STEINHAUER,[1] S.A. WHARTON,[1] AND D.C. WILEY[3]

[1]*National Institute for Medical Research, Mill Hill, London NW7 1AA, United Kingdom;* [2]*Laboratoire de Biologie Structurale, UMR 9920, CNRS-Université Paris-Sud, 91198 Gif-sur-Yvette Cedex, France;* [3]*Department of Biochemistry and Molecular Biology and Howard Hughes Medical Institute, Harvard University, Cambridge, Massachusetts 02138*

Enveloped viruses infect cells by binding to cell-surface receptors and then fusing their membranes with cellular membranes to deliver their genetic material into the cell. Fusion can occur at the cell surface as is the case, for example, for paramyxoviruses (see, e.g., Kohn 1965), but in many infections it involves interactions between virus membranes and the membranes of endosomes into which the receptor-bound viruses are transferred (see, e.g., Helenius et al. 1980). This is the case for influenza viruses for which the fusion potential of the receptor-binding membrane-fusion glycoprotein, the hemagglutinin (HA), is activated at endosomal pH (Maeda and Ohnishi 1980; Huang et al. 1981; White et al. 1981) in a process that involves extensive structural changes in the molecule. We present here observations on the nature of these changes that contribute to an understanding of their requirement for fusion activity and to considerations of the mechanisms of protein-mediated membrane fusion.

NATIVE HA STRUCTURE

HAs are trimers of molecular weight about 220,000, 135 Å long, and approximately triangular in cross-section, varying in radius from about 15 Å to 40 Å. Each monomer consists of two disulfide-linked glycopolypeptides, HA_1 and HA_2 (Compans et al. 1970; Schulze 1970; Laver 1971; Skehel and Schild 1971), produced during infection by cleavage of a precursor, HA_0 (Klenk et al. 1972; Skehel 1972; Stanley et al. 1973). Cleavage generates the carboxyl terminus of HA_1 and the amino terminus of HA_2 (Skehel and Waterfield 1975) and is necessary for infectivity (Klenk et al. 1975; Lazarowitz and Choppin 1975) and for membrane fusion activity (Huang et al. 1981; White et al. 1981). Largely because of similar requirements by fusion glycoproteins of other viruses (Homma and Ohuchi 1973; Scheid and Choppin 1974), similarities in the amino-terminal sequences at the sites of cleavage (Gething et al. 1978), and the membrane-fusion properties of synthetic peptide analogs of these sequences (Lear and de Grado 1987; Murata et al. 1987; Wharton et al. 1988a), the amino-terminal region of HA_2 has become known as the "fusion peptide." The three-dimensional structure of the HA from the influenza virus of the 1968 pandemic, A/Aichi/2/68, has been solved to 2.15 Å resolution (Wilson et al. 1981; Knossow et al. 1986; Watowich et al. 1994). Figure 1a is a diagram of a subunit which shows that the HA_1 chain (light blue in Fig. 1) extends from the base of the molecule near the virus membrane, through a fibrous stem, to a membrane-distal region rich in β-structure. This region contains the receptor-binding site (Weis et al. 1988) and the sites to which infectivity-neutralizing antibodies bind (Wiley et al. 1981). Returning to the fibrous region, the HA_1 chain terminates about 30 Å from the membrane. The most prominent features formed by the HA_2 chain are a hairpin-like structure consisting of two antiparallel α helices linked by an extended chain, and a membrane-proximal β sheet. The longer 52-residue α helices of the hairpins associate in the trimer to form a central membrane-distal 30-Å-long coiled coil. This extends to about 35 Å from the virus membrane where the helices separate to form a tripod-like structure that allows the central insertion of the amino-terminal region of HA_2, the fusion peptide. The shorter 18-residue α helix of each hairpin is packed between the longer α helices of adjacent subunits. The five-stranded β-sheet structure comprises two strands of β structure formed by the HA_2 chain at the membrane-proximal end of each α helix. The central fifth strand is contributed by the amino-terminal region of HA_1 as it extends away from the virus membrane.

HA IN THE FUSION pH CONFORMATION

The above information on the three-dimensional structure of native HA derives from analyses of crystals of the soluble ectodomain of HA, released from purified virus by digestion with the protease bromelain (Brand and Skehel 1972; Wilson et al. 1981). This fragment lacks the 46-residue-long carboxy-terminal region of HA_2 (Skehel and Waterfield 1975; Dopheide and Ward 1981; Wilson et al. 1981) that forms the hydrophobic membrane anchor of the complete glycoprotein and extends 11 residues internal to the virus membrane (Verhoeyen et al. 1980). It is, however, indistinguishable from the ectodomain of complete HA in subunit composition (Wiley et al. 1977), antigenicity (Daniels et al. 1983a), secondary structure (Flanagan and Skehel 1977), and electron microscopic appearance (Wrigley et al. 1983; Ruigrok et al. 1986b). Its preparation involves extensive bromelain digestion, and at neutral

pH it is resistant to further proteolysis. At the pH of membrane fusion, however, the ectodomain self-aggregates to form protein micelles that are sensitive to proteolysis (Fig. 2) (Skehel et al. 1982; Doms et al. 1985). Endoproteinase LysC or trypsin digestion of the micelles cleaves HA_1 at Lys-27, a residue buried in native HA, to release the membrane-distal domain formed by HA_1 residues 28–328 as a soluble monomer (Skehel et al. 1982; Bizebard et al. 1995). Subsequent thermolytic digestion dissociates the residual HA_2 micelles (Fig. 2) by removing initially the amino-terminal 23 residues of HA_2 and eventually the 37 amino-terminal residues (Daniels et al. 1983b; Ruigrok et al. 1988). The soluble product is trimeric and contains HA_2, residues 38–175, disulfide-linked ($HA_1$14–$HA_2$137) to the amino-terminal peptide of HA_1, residues 1–27. The derivation and properties of these two soluble fragments of HA in the fusion-pH conformation are described diagrammatically in Figure 1. As in the case of the soluble HA ectodomain, their structures have been solved crystallographically (Bullough et al. 1994; Bizebard et al. 1995).

THE MEMBRANE-DISTAL GLOBULAR DOMAIN, HA_1 RESIDUES 28-328

Chemical cross-linking of the soluble fragment HA_1 28-328 released proteolytically from fusion-pH HA micelles indicated that it is monomeric (Ruigrok et al. 1988). Following deglycosylation by digestion with N-glycosidase F and endoglycosidase H, the fragment formed a soluble complex with a Fab of known structure derived from a virus infectivity-neutralizing monoclonal antibody (Bizebard et al. 1994, 1995). The three-dimensional structure of the crystalline complex was determined at 3.3 Å resolution. In the crystal as in solution, the fragment is monomeric, and between HA_1 43 and HA_1 309 it retains the structure that it adopts in native HA (Fig. 1). This is consistent with observations that the fragment binds anti-HA monoclonal antibodies other than those that interact near the membrane-distal trimeric interface (Daniels et al. 1983a), its secondary structure is indistinguishable by circular dichroism (CD) from that deduced in the intact molecule (Skehel et al. 1982; Ruigrok et al. 1986a; Wharton et al. 1988b), and receptor-binding activity is retained by HA in the fusion-pH conformation (Daniels et al. 1983a; Sauter et al. 1989). The amino-terminal and carboxy-terminal strands, HA_1 28-42 and HA_1 310-328, respectively, are disordered.

THE SOLUBLE FRAGMENT PREPARED FROM THE FUSION-pH-INDUCED HA MICELLE BY THERMOLYTIC DIGESTION: HA_2 38-175:HA_1 1-27

Chemical cross-linking indicated that this fragment remains trimeric (Ruigrok et al. 1988), but the crystal structure revealed extensive reorganization of these regions by comparison with their positions in the native molecule (Bullough et al. 1994). The color coding of the regions in Figure 1 is designed to illustrate the nature of these changes. In the fusion-pH conformation, the amino-terminal region of HA_2, the fusion peptide, and two β strands to which it is connected (white, Fig. 1) form an extension of unknown structure to a new 67-residue α helix (HA_2 38-105). In the fusion-pH trimer, this α helix forms a 100-Å-long coiled coil, the carboxy-terminal 30 residues of which (HA_2 76-105, yellow, Fig. 1) are the only residues of the fragment to maintain their neutral-pH structure. They are preceded in the α helix by residues HA_2 58-75 (orange, Fig. 1), which formed the extended chain linking the two antiparallel α helices of the native helical hairpin and the shorter α helix of the hairpin (HA_2 38-57, red, Fig. 1) also translated through about 100 Å from its position in native HA and rotated 180°. Carboxy-terminal to this new helix, residues HA_2 106-112 (green, Fig. 1), which formed part of the longer helix of native HA_2, refold to invert the remainder of the native helix (HA_2 113-129, blue, Fig. 1), which remains helical in its new orientation, together with three strands of the native five-stranded β sheet and short α helices carboxy-terminal to them (magenta, Fig. 1). Beyond residue 162, HA_2 is disordered in the crystal.

To summarize: In response to the pH of fusion in endosomes during infection or in vitro, concerted changes in HA structure occur (Fig. 3). These include:

1. Release of the fusion peptide from its buried native position and its relocation to the membrane-distal tip of a 100-Å-long triple-stranded coiled coil.
2. Formation of this coiled coil as a membrane-distal extension of the central 30 Å coiled coil of native HA by refolding the chain linking the two α helices of the native α helical hairpin and translocating the shorter helix to the top of the extension.
3. De-trimerization of the HA_1 membrane-distal globular domains that otherwise retain their native structure and remain disulfide-linked through the elongated amino-terminal chain of HA_1 to the rearranged trimer.
4. Inversion, en bloc, of the carboxy-terminal segment of the long central helix of native HA and the remainder of the membrane-proximal native HA_2 structure.

These interpretations of the fusion-pH conformational change are consistent with proposals of a direct role in fusion for the hydrophobic fusion peptide (for review, see Wiley and Skehel 1987). As the amino terminus of the newly formed coiled coil, it would be projected toward the endosomal membrane, perhaps interacting with it to form a bridge with the virus membrane. If required for fusion, the gap between the two membranes may be narrowed by orienting the bridge parallel to them. This would seem to be possible if the interpretations of flexibility at both ends of the reorganized HA_2 chain are correct.

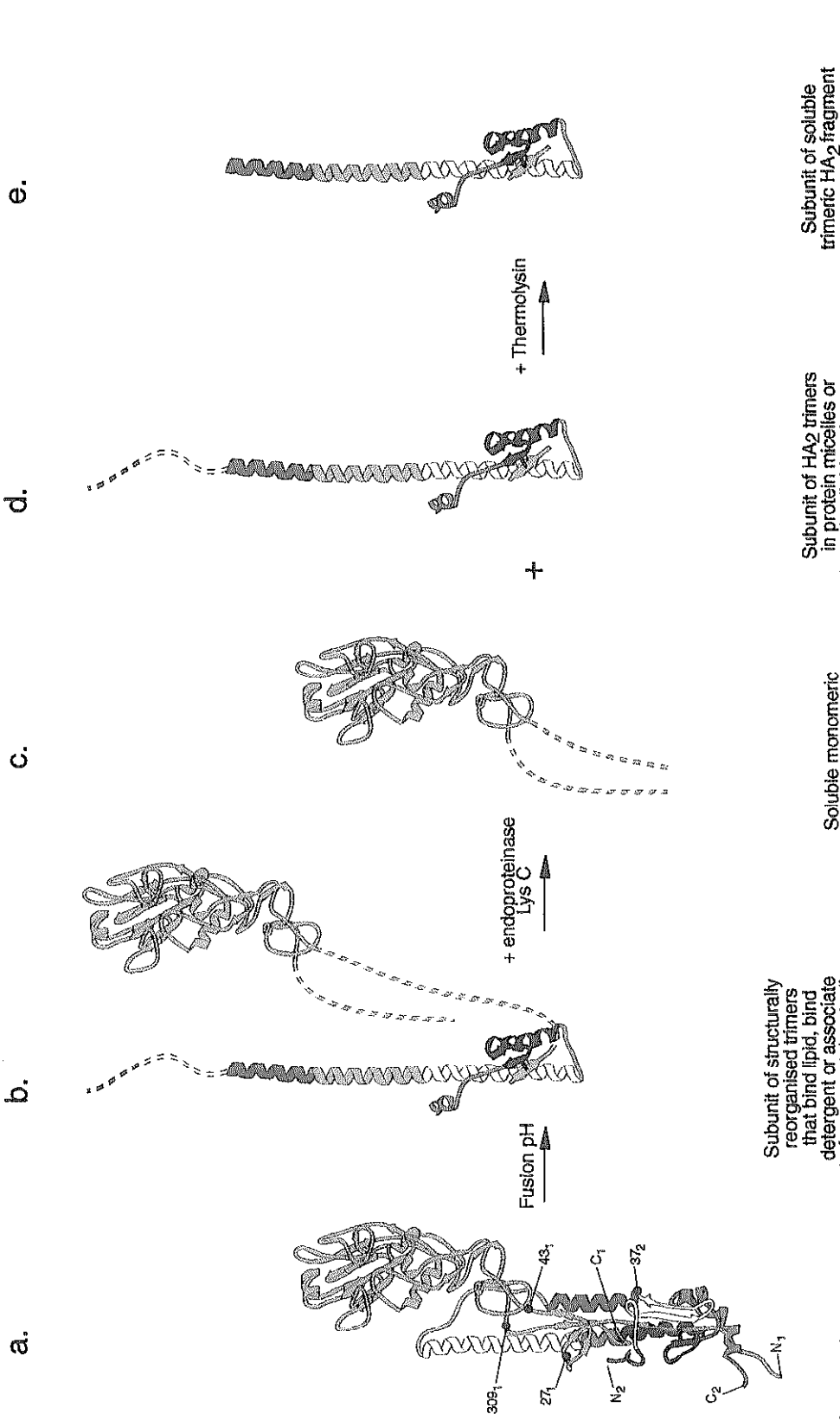

Figure 1. Diagrams of the structure of (*a*) a subunit of the native HA trimer (Wilson et al. 1981), indicating the amino and carboxyl termini of the HA_1 and HA_2 chains, N_1, C_1, and N_2, C_2, the sites of proteolytic digestion exposed at fusion pH, HA_1 residue 27, 27_1, and HA_2 residue 37, 37_2 recognized by endoproteinase LysC and thermolysin, respectively; and HA_1 residues 43_1 and 309_1 beyond which the HA_1 domain is disordered in the Fab-HA_1 28-328 crystal structure. The HA_1 chain is light blue, the HA_2 chain is color-coded to explain the fusion-pH-induced changes in structure. (*b*) The structure of a subunit of the fusion-pH trimer constructed diagramatically by adding the HA_1 28-328 domain structure (*c*) to the HA_2 38-175: HA_1 1-27 thermolytic fragment structure (*e*). The discontinuous lines indicate components of the structures that are unknown. (*c,d*) Structures of the fragments resulting from endoproteinase LysC digestion of HA micelles at HA_1 residue 27. The structure *c* was determined as a complex with a monoclonal antibody Fab fragment (Bizebard et al. 1995); the structure *d* was deduced from *e*, a subunit of the soluble trimer prepared from the HA_2 micelle by thermolytic digestion at HA_2 residue 37 (Bullough et al. 1994).

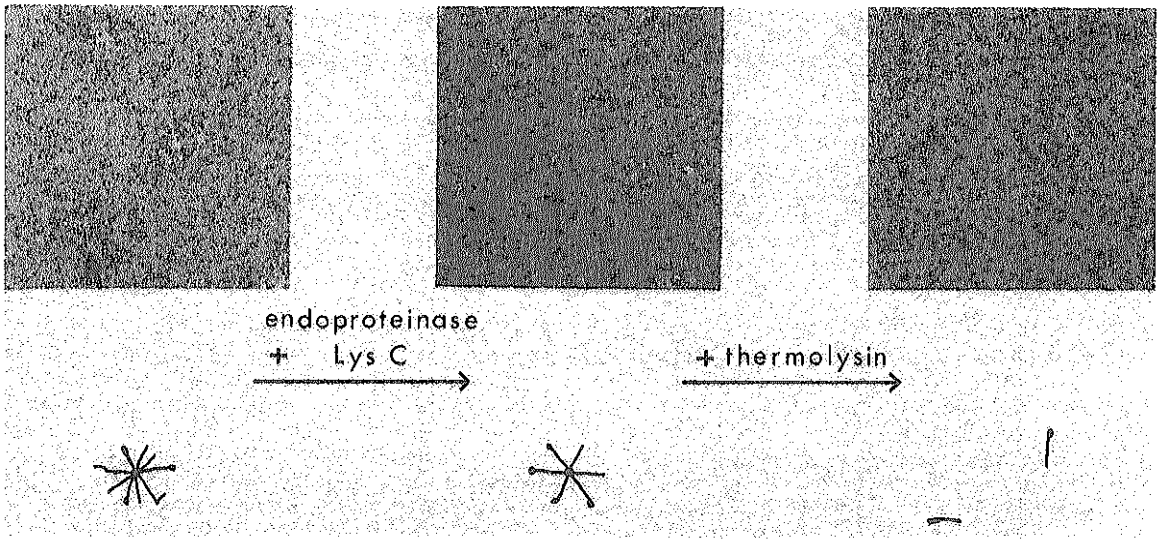

Figure 2. Electron micrographs of HA micelles, HA_2 micelles, and thermolytic fragment HA_2 38-175: HA_1 1-27 noted in Fig. 1, *b*, *d*, and *e*, respectively. Soluble, bromelain-released HA incubated at fusion pH forms HA micelles (*left*); endoproteinase LysC digestion of HA micelles forms HA_2 micelles (*center*). Thermolytic digestion of HA_2 micelles produces the soluble fragment HA_2 38-175: HA_1 1-27 (*right*). Negative staining with 1% sodium silicotungstate and protein preparations were carried out as described in Wharton et al. (1995). The arrowed components are sketched below the micrographs.

FUSION pH MUTANTS

HA_2 in the fusion-pH conformation is more stable than native HA, as judged by its susceptibility to proteolysis and by spectroscopically detected changes in secondary structure as a function of temperature (Ruigrok et al. 1986a, 1988). This suggests that the cleavage of the precursor HA_0 is designed to produce a comparatively unstable HA primed for the fusion-pH-induced transition to a fusion-active form.

Analyses of mutant HAs that fuse membranes at higher pH than wild type led to the conclusions that

Figure 3. A diagram of the fusion-pH HA trimer constructed from the HA_1 (*blue*) and HA_2 (*red*) structures described by Bizebard et al. (1995) and Bullough et al. (1994), to show the central trimeric coiled coil and the detrimerized HA_1 membrane-distal domains. The structures represented by the discontinuous lines are unknown, as is the relative orientation of the different domains.

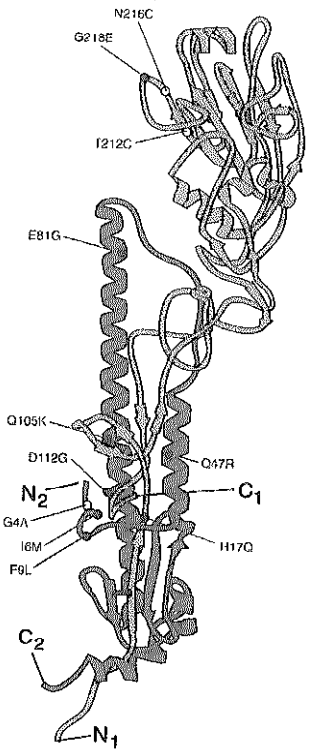

Figure 4. A subunit of native HA to show the locations throughout the length of the molecule of amino acid substitutions (*filled circles*) that increase the pH of fusion by mutant HAs (Daniels et al. 1985, 1987). The open circles indicate the positions of site-specific changes made in studies of the fusion peptide (Gething et al. 1986; Steinhauer et al. 1995) and to disulfide cross-link the trimer in the membrane-distal domain (Godley et al. 1992).

the amino acid substitutions that they contain further destabilize the neutral-pH structure relative to the fusion-pH form and, in addition, that their distribution throughout the length of the trimer was indicative of extensive structural change at the pH of fusion (Daniels et al. 1985, 1987). Both conclusions are now supported by comparison of the molecular locations of the residues in native and fusion-pH HA structures (Bullough et al. 1994). There are two groups of mutants (Fig. 4): (1) those which contain substitutions that appear to destabilize the location of the HA_2 amino-terminal fusion peptide either by loss of hydrogen bonds to polar atoms, e.g., HA_2 D112G and HA_1 H17Q or by causing unfavorable packing interactions e.g., HA_2 I6M and HA_2 F9L; and (2) those which appear to involve loss or distortion of interactions in the interfaces between the chains and subunits of the trimer, distant from the fusion peptide and throughout the length of the molecule, e.g., HA_2 Q47R, HA_2 Q105K, HA_2 E81G, and HA_1 G218E. All of the residues identify interactions that are lost in the transition to the fusion-pH structure; by comparison, mutations in the native coiled coil have not been selected.

The functional significance of the structural changes is supported by these genetic observations and has been reinforced by site-specific mutagenesis in the region of the fusion peptide, e.g., HA_2 G4E or G4A (Gething et al. 1986; Steinhauer et al. 1995), and in the membrane-distal region of HA_1 (Godley et al. 1992). In the latter case especially, a requirement for reorganization of the membrane-distal globular domains was clearly shown by the introduction of intersubunit disulfide bonds through HA_1 T212C and HA_1 N216C substitutions, to covalently cross-link the trimer. These bonds prevented the fusion-pH-induced changes in structure and prevented fusion; their reduction allowed both structural changes and membrane fusion to proceed.

ELECTRON MICROSCOPY

The conclusions drawn from the X-ray structures also explain a number of the features of lower-resolution electron microscopy (EM) images of HA in the fusion-pH conformation and proteolytic fragments derived from it. The disorganized and elongated projections from HA micelles formed when membrane-anchorless bromelain-solubilized HA is incubated at fusion pH (Fig. 2) (Ruigrok et al. 1986b) can, for example, be interpreted to represent detrimerized HA_1 membrane-distal domains tethered to the HA_2 trimer by extended and flexible amino-terminal chains of HA_1. The terminal knobs on the HA_2-micelle projections (Fig. 2) (Ruigrok et al. 1988) can also be interpreted as representing the inverted region of HA_2 (blue and magenta, Fig. 1); the knob at one end of the thermolytic fragment of HA_2 (Ruigrok et al. 1988) can be identified similarly.

The overall dimensions of this fragment deduced from EM images agree well with those provided by the X-ray studies; in particular, they indicate a length of 105 Å, in close agreement with the length of the coiled coil. This measurement precluded a simple application of the results of amino acid sequence-based structure prediction to the fusion-pH structure of HA_2. These methods were applied to HA sequences when they first became available (Ward and Dopheide 1980) before the three-dimensional structure of native HA was known, and suggested an approximately 90-residue, 135-Å-long α-helical coiled-coil component of HA_2 rather than the α-helical hairpin structure that HA_2 was subsequently found to adopt in native HA. Similar predictions, together with analyses of CD spectra of synthetic peptide analogs of parts of HA_2, later led to the proposal that HA_2 rearranges to form the predicted 135-Å-long coiled coil in the fusogenic state (Carr and Kim 1993). In this case, although there is indeed a structural rearrangement at low pH, the inverted hairpin structure that forms one end of the fusion-pH-induced HA_2 coiled coil was not anticipated, and the proposal was inconsistent with EM measurements of the length of the thermolytic fragment derived from fusion-pH HA (Ruigrok et al. 1986b, 1988).

EM analyses of HA have also been useful in studies of the fusion-pH structures of complete HA and fragments that contain fusion peptides or membrane-anchor regions, which in some cases, because of their tendency to form micelles, have not been crystallized. EM of one such fragment, derived as an initial thermolytic digestion product of HA_2, 14 residues longer than the fragment used in the X-ray studies, had a length of 130 Å compared with 110 Å for the crystalline fragment (Ruigrok et al. 1988). These measurements, together with those of the length of HA_2 micelles (Ruigrok et al. 1986b), are the basis for the HA_2 amino-terminal extension shown in Figure 1b and d and for the conclusion that the fusion peptide is at the top of the coiled coil.

Analysis of virosomes containing HA_2 (Fig. 5) showed that the structure of HA_2 projecting from the membrane is indistinguishable by EM from that of the thermolytic fragment of HA_2, indicating that there are no detectable structural consequences of the lack of a carboxy-terminal membrane anchor or of an amino-terminal fusion peptide for the conformation of HA_2 at fusion pH (Wharton et al. 1995). Further probing of these structures with monoclonal antibodies that specifically bound at fusion pH to the refolded section of the longer native α helix, HA_2 106-112 (green, Fig. 1), clearly showed the membrane-distal location of this knob-forming region of the molecule. These observations also indicate that the fusion peptide is associated with the virosome membrane, which is consistent with results from photoactivated-phospholipid labeling of HA_2 in virus membranes (Weber et al. 1994).

HA_2 in this orientation, therefore, appears to be associated with the virosome membrane through both its carboxy-terminal membrane anchor and its amino-

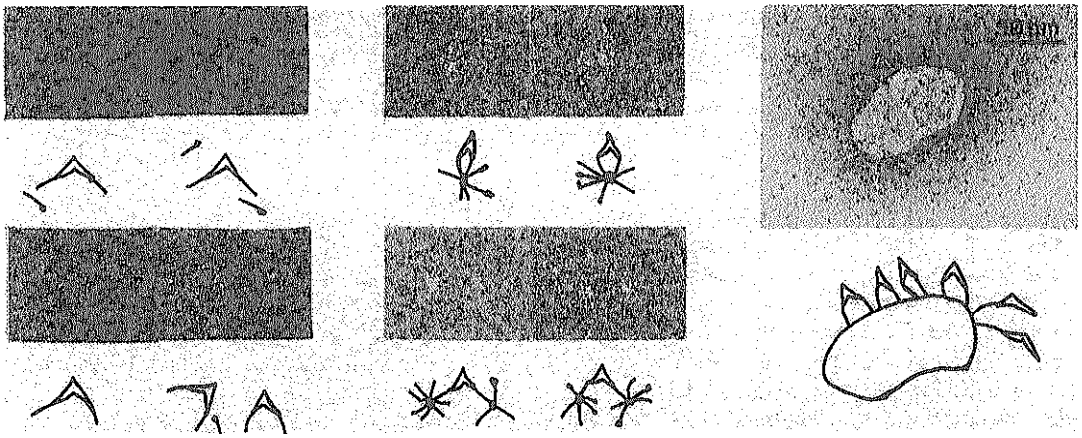

Figure 5. Electron micrographs of HA_2 in virosome-antibody complexes (*right*), HA_2 micelle-antibody complexes (*center*), and HA_2 thermolytic fragment-antibody complexes (*left*) together with diagrams of the complexes (antibodies as open shapes) to show the location of the antibody-binding site, and consequently, the orientation of fusion-pH HA_2 in the respective complexes. The monoclonal antibody used, LC89, recognizes HA_2 residue 107 in the refolded turn at the carboxyl terminus of the fusion-pH coiled coil that defines its binding site. It binds to the membrane-distal region of HA_2 in virosomes and to the projected ends of HA_2 in micelles indicating the membrane location of the carboxy-terminal membrane anchor and the amino-terminal fusion peptide of HA_2 in virosomes and the central location of the fusion peptide in HA_2 micelles (Wharton et al. 1995).

terminal fusion peptide, implying that rotation of complete HA_2 occurs when virosomes, or indeed viruses, are incubated at fusion pH in the absence of a target membrane. This process, which would seem automatically to inactivate HA fusion capacity, reflects the flexibility of the carboxy-terminal, membrane-proximal region of HA_2, and the inverted structure may represent an orientation adopted by HA with the formation of a single membrane at the completion of fusion.

ACKNOWLEDGMENTS

We thank Lesley Calder, Alan Douglas, Rose Gonsalves, and David Stevens for excellent assistance. This work was supported by the Medical Research Council, National Institutes of Health (A1-13654 to D.C.W.), CNRS, and the European Economic Community. D.C.W. is an investigator with the Howard Hughes Medical Institute.

REFERENCES

Bizebard, T., R. Daniels, R. Kahn, B. Golinelli-Pimpaneau, J.J. Skehel, and M. Knossow. 1994. Refined three-dimensional structure of the Fab fragment of a murine 1gG1, λ antibody. *Acta Crystallogr.* **D50:** 768.

Bizebard, T., B. Gigant, P. Rigolet, B. Rasmussen, O. Diat, P. Bösecke, S.A. Wharton, J.J. Skehel, and M. Knossow. 1995. Structure of influenza virus haemagglutinin complexed with a neutralizing antibody. *Nature* **376:** 92.

Brand, C.M. and J.J. Skehel. 1972. Crystalline antigen from the influenza virus envelope. *Nat. New Biol.* **238:** 145.

Bullough, P.A., F.M. Hughson, J.J. Skehel, and D.C. Wiley. 1994. The structure of influenza haemagglutinin at the pH of membrane fusion. *Nature* **371:** 37.

Carr, C.M. and P.S. Kim. 1993. A spring-loaded mechanism for the conformational change of influenza hemagglutinin. *Cell* **73:** 823.

Compans, R.W., H.-D. Klenk, L.A. Caliguiri, and P.W. Choppin. 1970. Influenza virus proteins 1. Analysis of polypeptides of the virion and identification of spike glycoproteins. *Virology* **42:** 880.

Daniels, R.S., A.R. Douglas, J.J. Skehel, and D.C. Wiley. 1983a. Analyses of the antigenicity of influenza haemagglutinin at the pH optimum for virus-mediated membrane fusion. *J. Gen. Virol.* **64:** 1657.

Daniels, R.S., A.R. Douglas, J.J. Skehel, M.D. Waterfield, I.A. Wilson, and D.C. Wiley. 1983b. Studies of the influenza virus haemagglutinin in the pH5 conformation. In *The origin of pandemic influenza viruses* (ed. W.G. Laver), p. 1. Elsevier, New York.

Daniels, R.S., J.C. Downie, A.J. Hay, M. Knossow, J.J. Skehel, M.L. Wang, and D.C. Wiley. 1985. Fusion mutants of the influenza virus hemagglutinin glycoprotein. *Cell* **40:** 431.

Daniels, R.S., S. Jeffries, P. Yates, G.C. Schild, G.N. Rogers, J.C. Paulson, S.A. Wharton, A.R. Douglas, J.J. Skehel, and D.C. Wiley. 1987. The receptor-binding and membrane-fusion properties of influenza virus variants selected using anti-haemagglutinin monoclonal antibodies. *EMBO J.* **6:** 1459.

Doms, R.W., A.H. Helenius, and J.M. White. 1985. Membrane fusion activity of the influenza virus hemagglutinin: The low pH-induced conformational change. *J. Biol. Chem.* **260:** 2973.

Dopheide, T.A.A. and C.W. Ward. 1981. The location of the bromelain-cleavage site in a Hong Kong influenza virus hemagglutinin. *J. Gen. Virol.* **52:** 367.

Flanagan, M.T. and J.J. Skehel. 1977. The conformation of influenza virus haemagglutinin. *FEBS Lett.* **80:** 57.

Gething, M.J., J.M. White, and M.D. Waterfield. 1978. Purification of the fusion protein of Sendai virus: Analysis of the NH_2-terminal sequence generated during precursor activation. *Proc. Natl. Acad. Sci.* **75:** 2737.

Gething, M.J., R.W. Doms, D. York, and J. White. 1986.

Studies on the mechanism of membrane fusion: Site-specific mutagenesis of the hemagglutinin of influenza virus. *J. Cell Biol.* **102:** 11.

Godley, L., J. Pfeifer, D. Steinhauer, B. Ely, G. Shaw, R. Kaufmann, E. Suchanek, C. Pabo, J.J. Skehel, D.C. Wiley, and S. Wharton. 1992. Introduction of intersubunit disulfide bonds in the membrane-distal region of the influenza hemagglutinin abolishes membrane fusion activity. *Cell* **68:** 635.

Helenius, A., J. Kartenbeck, K. Simons, and E. Fries. 1980. On the entry of Semliki forest virus into BHK-21 cells. *J. Cell Biol.* **84:** 404.

Homma, M. and M. Ohuchi. 1973. Trypsin action on the growth of Sendai virus in tissue culture cells. III. Structural difference of Sendai viruses grown in eggs and tissue culture cells. *J. Virol.* **12:** 1457.

Huang, R.T.C., R. Rott, and H.-D. Klenk. 1981. Influenza viruses cause hemolysis and fusion of cells. *Virology* **110:** 243.

Klenk, H.-D., C. Scholtissek, and R. Rott. 1972. Inhibition of glycoprotein brosynthesis of influenza virus by D-glucosamine and 2-deoxy-D-glucose. *Virology* **49:** 723.

Klenk, H.-D., R. Rott, M. Orlich, and J. Blodorn. 1975. Activation of influenza A viruses by trypsin treatment. *Virology* **68:** 426.

Knossow, M., M. Lewis, D. Rees, I.A. Wilson, J.J. Skehel, and D.C. Wiley. 1986. The refinement of the haemagglutinin membrane glycoprotein of influenza virus. *Acta Crystallogr.* **B42:** 627.

Kohn, A. 1965. Polykaryocytosis induced by Newcastle disease virus in monolayers of animal cells. *Virology* **26:** 228.

Laver, W.G. 1971. Separation of two polypeptide chains from the hemagglutinin subunit of influenza virus. *Virology* **45:** 275.

Lazarowitz, S.G. and P.W. Choppin. 1975. Enhancement of the infectivity of influenza A and B viruses by proteolytic cleavage of the hemagglutinin polypeptide. *Virology* **68:** 440.

Lear, J.D. and W.F. de Grado. 1987. Membrane binding and conformational properties of a peptide representing the amino terminus of influenza virus HA_2. *J. Biol. Chem.* **262:** 6500.

Maeda, T. and S. Ohnishi. 1980. Activation of influenza virus by acidic media causes hemolysis and fusion of erythrocytes. *FEBS Lett.* **122:** 283.

Murata, M., Y. Sugahara, S. Takahashi, and S.I. Ohnishi. 1987. pH-dependent membrane fusion activity of a synthetic twenty amino acid peptide with the same sequence as that of the hydrophobic segment of influenza virus haemagglutinin. *J. Biochem.* **102:** 957.

Ruigrok, R.W.H., S.R. Martin, S.A. Wharton, J.J. Skehel, P.M. Bayley, and D.C. Wiley. 1986a. Conformational changes in the hemagglutinin of influenza virus which accompany heat-induced fusion of virus with liposomes. *Virology* **155:** 484.

Ruigrok, R.W.H., N.G. Wrigley, L.J. Calder, S. Cusack, S.A. Wharton, E.B. Brown, and J.J. Skehel. 1986b. Electron microscopy of the low pH structure of influenza virus haemagglutinin. *EMBO J.* **5:** 41.

Ruigrok, R.W.H., A. Aitken, L.J. Calder, S.R. Martin, J.J. Skehel, S.A. Wharton, W. Weis, and D.C. Wiley. 1988. Studies on the structure of influenza virus haemagglutinin at the pH of membrane fusion. *J. Gen. Virol.* **69:** 2785.

Sauter, N.K., M.D. Bednarski, B.A. Wurzburg, J.E. Hanson, G.M. Whitesides, J.J. Skehel, and D.C. Wiley. 1989. Hemagglutinins from two influenza virus variants bind to sialic acid derivatives with millimolar dissociation constants: A 500-MHz proton nuclear magnetic resonance study. *Biochemistry* **28:** 8388.

Scheid, A. and P.W. Choppin. 1974. Identification of biological activities of paramyxovirus glycoproteins. Activation of cell fusion, hemolysis, and infectivity by proteolytic cleavage of an inactive precursor protein of Sendai virus. *Virology* **57:** 475.

Schulze, I.T. 1970. The structure of influenza virus 1. The polypeptides of the virion. *Virology* **42:** 890.

Skehel, J.J. 1972. Polypeptide synthesis in influenza virus infected cells. *Virology* **49:** 23.

Skehel, J.J. and G.C. Schild. 1971. The polypeptide composition of influenza A viruses. *Virology* **44:** 396.

Skehel, J.J. and M.D. Waterfield. 1975. Studies on the primary structure of the influenza virus haemagglutinin. *Proc. Natl. Acad. Sci.* **72:** 93.

Skehel, J.J., P.M. Bayley, E.B. Brown, S.R. Martin, M.D. Waterfield, J.M. White, I.A. Wilson, and D.C. Wiley. 1982. Changes in the conformation of influenza virus hemagglutinin at the pH optimum of virus-mediated membrane fusion. *Proc. Natl. Acad. Sci.* **79:** 968.

Stanley, P., S.S. Gandhi, and D.O. White. 1973. The polypeptides of influenza virus VII: Synthesis of the hemagglutinin. *Virology* **53:** 92.

Steinhauer, D.A., S.A. Wharton, J.J. Skehel, and D.C. Wiley. 1995. Studies on the membrane fusion activities of "fusion peptide" mutants of influenza hemagglutinin. *J. Virol.* **69:** 6643.

Verhoeyen, M., R. Fang, N. Min Jou, R. Devos, P. Huylebroeck, E. Saman, and W. Fiers. 1980. Antigenic drift between the haemagglutinin of the Hong Kong influenza strain A/Aichi/2/68 and A/Victoria/3/75. *Nature* **286:** 771.

Ward, C.W. and T.A.A. Dopheide. 1980. Influenza virus hemagglutinin. Structural predictions suggest that fibrillar appearance is due to the presence of a coiled-coil. *Aust. J. Biol. Sci.* **33:** 449.

Watowich, S.J., J.J. Skehel, and D.C. Wiley. 1994. Crystal structures of influenza virus hemagglutinin in complex with high-affinity receptor analogs. *Structure* **2:** 719.

Weber, T., G. Paesold, C. Galli, R. Mischler, G. Semeuza, and J. Brunner. 1994. Evidence for H^+-induced insertion of influenza hemagglutinin HA_2 N-terminal segment into viral membrane. *J. Biol. Chem.* **269:** 18353.

Weis, W., J. Brown, S. Cusack, J.C. Paulson, J.J. Skehel, and D.C. Wiley. 1988. The structure of the influenza virus haemagglutinin complexed with its receptor, sialic acid. *Nature* **33:** 426.

Wharton, S.A., S.R. Martin, R.W.H. Ruigrok, J.J. Skehel, and D.C. Wiley. 1988a. Membrane fusion by peptide analogs of influenza virus haemagglutinin. *J. Gen. Virol.* **69:** 1847.

Wharton, S.A., L.J. Calder, R.W.H. Ruigrok, J.J. Skehel, D.A. Steinhauer, and D.C. Wiley. 1995. Electron microscopy of antibody complexes of influenza virus haemagglutinin in the fusion pH conformation. *EMBO J.* **14:** 240.

Wharton, S.A., R.W.H. Ruigrok, S.R. Martin, J.J. Skehel, P.M. Bayley, W. Weis, and D.C. Wiley. 1988b. Conformational aspects of the acid-induced fusion mechanism of influenza virus hemagglutinin. Circular dichroism and fluorescence studies. *J. Biol. Chem.* **263:** 4474.

White, J., K. Matlin, and A. Helenius. 1981. Cell fusion by Semliki forest, influenza and vesicular stomatitis viruses. *J. Cell. Biol.* **89:** 674.

Wiley, D.C. and J.J. Skehel. 1987. The structure and function

of the hemagglutinin membrane glycoprotein of influenza virus. *Annu. Rev. Biochem.* **56:** 365.

Wiley, D.C., I.A. Wilson, and J.J. Skehel. 1981. Structural identification of the antibody-binding sites of Hong Kong influenza haemagglutinin and their involvement in antigenic variation. *Nature* **289:** 373.

Wiley, D.C., J.J. Skehel, and M.D. Waterfield. 1977. Evidence from studies with a cross-linking reagent that the haemagglutinin of influenza is a trimer. *Virology* **79:** 446.

Wilson, I.A., J.J. Skehel, and D.C. Wiley. 1981. Structure of the haemagglutinin membrane glycoprotein of influenza virus at 3Å resolution. *Nature* **289:** 366.

Wrigley, N.G., E.B. Brown, R.S. Daniels, A.R. Douglas, J.J. Skehel, and D.C. Wiley. 1983. Electron microscopy of influenza haemagglutinin-monoclonal antibody complexes. *Virology* **131:** 308.